University of Tennessee, Knoxville
TRACE: Tennessee Research and Creative Exchange

Masters Theses | Graduate School

8-2020

Sustained Release of Persulfate and Iron(II) Ions from Inert Inorganic Materials for Groundwater Remediation

Peter Pham
ppham2@vols.utk.edu

Follow this and additional works at: https://trace.tennessee.edu/utk_gradthes

 Part of the Analytical Chemistry Commons, and the Environmental Chemistry Commons

Recommended Citation

Pham, Peter, "Sustained Release of Persulfate and Iron(II) Ions from Inert Inorganic Materials for Groundwater Remediation. " Master's Thesis, University of Tennessee, 2020.
https://trace.tennessee.edu/utk_gradthes/6260

This Thesis is brought to you for free and open access by the Graduate School at TRACE: Tennessee Research and Creative Exchange. It has been accepted for inclusion in Masters Theses by an authorized administrator of TRACE: Tennessee Research and Creative Exchange. For more information, please contact trace@utk.edu.

To the Graduate Council:

I am submitting herewith a thesis written by Peter Pham entitled "Sustained Release of Persulfate and Iron(II) Ions from Inert Inorganic Materials for Groundwater Remediation." I have examined the final electronic copy of this thesis for form and content and recommend that it be accepted in partial fulfillment of the requirements for the degree of Master of Science, with a major in Chemistry.

Dr. Ziling Xue, Major Professor

We have read this thesis and recommend its acceptance:

Dr. Ziling Xue, Dr. Bhavya Sharma, Dr. Bin Zhao

Accepted for the Council:
Dixie L. Thompson

Vice Provost and Dean of the Graduate School

(Original signatures are on file with official student records.)

Sustained Release of Persulfate and Iron(II) Ions from Inert Inorganic Materials for Groundwater Remediation

A Thesis Presented for the

Master of Science

Degree

The University of Tennessee, Knoxville

Peter T. Pham

August 2020

Dedication

To my mother and father who made me the person I am today and to my fiancé, Vy Nguyen who has continuously supported me throughout this journey.

Acknowledgement

Firstly, I would like to thank my advisor Dr. Ziling (Ben) Xue who accepted me with open arms as one of his mentees in the analytical division of his lab. During my time at UTK, Dr. Xue has built me up to be a proper researcher. He has done so by playing an important role in the development of my researching, critical thinking, and communication skills. Furthermore, I thank Dr. Xue for showing me his utmost support for me during difficult times. I would like to also acknowledge Dr. Edmund Perfect, Dr. Bin Zhao, and Dr. Bhavya Sharma for agreeing to be my committee members to witness my worth as a chemist and for allowing me to improve upon my weaknesses.

Secondly, I would like to thank Dr. Kim Carter and Dr. Angel Palomino of the UT Department of Environmental and Civil Engineering, for the collaboration of my research project. They have provided me with fresh new insight into our research problem.

As for my colleagues, I would like to thank Dr. Roberto Federico-Perez for showing me the ropes around the lab. During his time here, Dr. Federico-Perez stood in as a secondary mentor who taught me numerous techniques and methods which I plan to apply in the near future. I would also like to thank Michael C. Orick, Yuanjun Song, Max Mortense and Prof. Siris Laursen for help with the BET studies. I thank Dr. Shelby Stavretis, Dr. Duncan Moseley, Zhiming Liu, Clay Mings, Chelsea Widener, Pagnareach Tin, Alex Bone, and Brian Kettell for their contributions to the foundation of a healthy work environment in the Xue lab.

Finally, I would like to thank Bryan Casale, Brandon Colon, Zhiming Liu, Evan Lewoczko for their companionship and for making my job a more enjoyable experience. In addition, I thank my friends and family outside of UTK for their support which includes

my best friend, Tuan Le, my eldest sister, Paula Pham, mother Phuong Tran, father Khanh Pham, and my other half, Vy Nguyen.

Abstract

Contamination of groundwater, initiated from years of human negligence, continues to persist despite major advancements in water remediation technologies. The generated groundwater plumes can continuously replenish contaminants such as dense nonaqueous phase liquids (DNAPLs) through the aid of slow-moving water. Thus, long-term treatment of this flow system has proven to be problematic. A selection of sophisticated sustained diffusion technologies is needed to help prevent further damage to this prominent freshwater source.

Here, a novel in-situ chemical oxidation (ISCO) method was designed to incorporate persulfate into silica mediums such as zeolite, diatom, and silica flour for the treatment of groundwater contaminants at polluted sites. By controlling the release of a strong oxidant solely through inorganic materials, the oxidizing potential is preserved in contrast to being released through organic mediums. Several methods of making the pellets as well as different types of pellets with a range of release time for persulfate have been developed, offering a selection of both methods and pellets for the controlled release of persulfate. These methods typically use an organic material such as candle wax or a polymer as the support in the pellets. Since the support materials are organic, they consume the released persulfate. In the current work, inorganic sol-gel, consisting of primarily silicon dioxide, was used as an adhesive for added internal support for the pellets. A chlorinated DNAPL known as trichloroethylene (TCE) was selected for testing this method. The feasibility of controlling the release of ferrous sulfate as an activator for persulfate was also briefly investigated. Batch treatment of 15 mg L^{-1} of TCE solutions showed 73-99% degradation and a maximum persulfate release time of over 25 hours

from persulfate-containing pellets. Successful treatment of a TCE-spiked Tennessee River water sample by persulfate and Fe^{2+} ions released from their respective pellets was demonstrated. Tests of the treated river water sample showed no detectable TCE by the silver chloride method. The purpose of this work is to show that these safe and inexpensive methods are potential prospects with further optimization and system scale-up for the continuous treatment of the groundwater in the near future.

This thesis is based in part on the following paper:

Pham, Peter T.; Federico-Perez, R. A.; Fine, K. L.; Matzek, L. W.; Carter, K. E.; Palomino, A. M.; Xue, Z.-L., Sustained Release of Persulfate from Inert Inorganic Materials for Groundwater Remediation, *Chemosphere* **2020**, *259*, 127508. https://doi.org/10.1016/j.chemosphere.2020.127508

Contributions of authors

Peter T. Pham: Investigation of Zeolite-, Diatom-, and Silica Flour-based Pellets, Methodology, Data Curation, Verification, Formal Analysis, Resources, Writing–Original Draft, Writing–Review & Editing, Visualization.

Roberto A. Federico-Perez: Investigation of Diatom-based Pellets, Methodology, Data Curation, Verification, Formal Analysis, Resources.

Kevin L. Fine: Investigation Silica Flour-based Pellets with P.H.P., Data Curation, Verification.

Laura W. Matzek: Methodology.

Kimberly E. Carter: Methodology, Resources, Writing–Original Draft, Writing–Review & Editing.

Angelica M. Palomino: Methodology, Resources, Writing–Original Draft, Writing–Review & Editing.

Zi-Ling Xue: Conceptualization with help by K.E.C. and A.M.P., Methodology, Supervision, Project Administration, Writing–Original Draft, Writing–Review & Editing.

Table of Contents

1. Introduction 1

2. Materials and Methods 9

2.1 General pellet preparation 11

2.2 Inorganic sol-gel synthesis 13

2.3 Release profiles of persulfate and Fe^{2+} pellets 13

2.4 TCE preparation and extraction 15

2.5 TCE determination 16

2.6 Chloride analysis 16

2.7 Characterization with nitrogen adsorption 18

3. Results and Discussion 19

3.1 Methods for pellet fabrication 20

3.2 Diffusion studies of pellets 23

3.2.1 Zeolite-based pellets 23

3.2.2 Diatomite-based pellets 25

3.2.3 Silica flour-based pellets 26

3.3 Fe^{2+} release profile 27

3.4 Control-released persulfate for TCE treatment studies 29

3.5 Chloride results 33

3.6 Pore size distribution studies 34

3.7 Preliminary studies of TCE treatments by released persulfate and Fe^{2+} ions from their respective pellets 37

4. Conclusion 39

References 42

Vita 52

List of Figures

Figure 1. (Left) Sol-gel formation at different pH with gradual lowering of pH (as solution is acidified) from sample **A** to **C**. pH 10 for **C**. (Middle-Right) Additional images of sample **C**. 6

Figure 2. Image of Method **B** persulfate-zeolite pellet (left), surface image of same pellet with 10x magnification (right). 21

Figure 3. Images of pellets by **Method B** (Left) vs. by **Method C** (Right). These were persulfate-zeolite pellets with a thin layer of sol-gel coating for the pellet on the right. 21

Figure 4. Persulfate release profiles of types **4** (uncoated) and **5** pellets (coated). Error bars were used to represent the results of 3 pellets. 24

Figure 5. Persulfate release profile of type **1** pellet (zeolite). Error bars were used to represent the results of 3 pellets. 24

Figure 6. Persulfate release profile of type **2** pellet (diatomite). Error bars were used to represent 3 pellets. 26

Figure 7. Persulfate release profile of type **3** pellet (silica flour). Error bars were used to represent results of 3 pellets. 27

Figure 8. Image of a type **6** pellet containing ferrous sulfate. 28

Figure 9. Fe^{2+} release profile of type **6** pellets. Error bars were used to represent results of 3 pellets. 28

Figure 10. Degradation of TCE in acetone-containing solution with type **1** pellet (zeolite). Error bars were used to represent results of 3 separate runs. 30

Figure 11. Degradation of TCE in acetone-containing solution with type **2** pellet (diatom). Error bars were used to represent results of 3 separate runs. 30

Figure 12. Degradation of TCE in acetone-containing solution with type **3** pellet (silica flour). Error bars were used to represent results of 3 separate runs. 31

Figure 13. Degradation of TCE in acetone-containing solution with type **4** pellet (zeolite/no sol gel). Error bars were used to represent results of 3 separate runs. Possible reason for the dip in TCE concentration at the 2-hour point is given on p. 29. 31

Figure 14. Degradation profile of TCE in acetone-free solution with type **1** pellet (zeolite). Error bars were used to represent results of 3 separate runs. 33

Figure 15. Nitrogen adsorption/desorption isotherm of a type **4** pellet. 35

Figure 16. BET surface area plot of a type **4** pellet. *Q* = quantity of N_2 adsorbed (mmol/g). 35

Figure 17. Incremental pore volume vs. pore width plot demonstrating the size distribution for the type **4** pellet. 36

Figure 18. Photos of the treatment process of a river water sample spiked with TCE, followed by silver chloride test. 37

1. Introduction

Groundwater contamination remains a pressing problem that could spiral out of control, creating detrimental damage to the aquatic environment and health risks for the overall public population. Of the numerous groundwater treatment options available, only a few have had limited success in effective removal of these toxic substances.[1-4] Some sources of human-induced contaminants range from heavy usage of pesticides to accidental chemical leakages from underground septic tanks. A notable group of contaminants commonly found in infected groundwater sites are known as dense non-aqueous phase liquids (DNAPLs).[5] These recalcitrant pollutants possess relatively high density and slight solubility in water, allowing them to ultimately reside underneath the water table after initial penetration of the soil subsurface. Consequently, plumes of contaminants are carried along a gradient and are constantly recharged with freshwater. During the recharge, contaminants are swept up once again from the contamination source concealed in bedrocks and produces a chronic supply for contaminant distribution. The complex nature of slow-moving groundwater coupled with the vexing properties of DNAPLs has proved challenging for conventional remediation technologies.[6-8] Trichloroethylene (TCE), a chlorinated compound commonly used as an industrial solvent, is one of the major contaminants found at the affected sites.[9-12] Due to its high volatility and carcinogenic properties, TCE was hastily disposed of with little to no regulation. As a result, many people have been exposed daily to these toxic chemicals through drinking water or by vapor intrusion from the soil. Thus, immediate response is required to combat against this ongoing contamination issue.[13,14]

Past approaches for water remediation include advanced oxidation processes (AOPs) and in-situ chemical oxidation (ISCO). AOPs are decomposition procedures

previously used in water treatment protocols to decompose organic contaminants in affected water sites. Some common, nonselective AOPs involve the use of hydrogen peroxide (H_2O_2) and ozone (O_3) through Fenton processes or activation by other methods [e.g., ultraviolet (UV) and sonolysis] to generate hydroxyl radical (OH•).[15,16] AOPs involving UV and sonolysis would not be adequate for subsurface groundwater treatment since the specialized equipment would be costly to maintain and very cumbersome to manage. Processes involving H_2O_2 and O_3 usually use excess of each reagent to degrade contaminants to safe levels. When deposited into groundwater systems, these oxidants react with dissolved organic matter (DOM) almost immediately before any contaminants can be degraded. As a result, a great quantity of the oxidant supply is wasted.[15,16] Thus, there is a need for reliable methods that maintain oxidants over a long period for proper contaminant treatment.

ISCO, recently differentiated from AOPs, are remediation technologies that involve injecting oxidants directly into the target site to degrade organic contaminants.[17-20] Common strong ISCO oxidizers used include H_2O_2, permanganate, percarbonate, and persulfate. Persulfate has become more popular in the recent years as it is relatively stable at ambient temperatures and possesses a longer shelf life when compared to H_2O_2.[21] As for limitations of permanganate, there are rapid reactions between the r species found in the subsurface (natural oxidant demand, NOD) and permanganate before contaminant oxidation occurs.[21] Several methods for activating persulfate have been investigated, including heat, UV, bases, mineral, peroxone, Fe^{2+} ions through a Fenton-like process as shown in Eq. 1, and chelated Fe^{2+} ions.[20,22-26]

$$S_2O_8^{2-} + Fe^{2+} \rightarrow SO_4^{\bullet-} + SO_4^{2-} + Fe^{3+} \quad \text{(Eq. 1)}$$

Remediation efforts involving the use of UV and heat are not feasible with system scale up since installment of the necessary machinery and maintenance would be quite expensive. Instead, Fe^{2+} ions are more suitable activating agents that theoretically provide a single electron to break the peroxyl bond in persulfate to form reactive sulfate radicals ($SO_4^{\bullet-}$) as shown in Eq. 1. Like hydroxyl radicals, these sulfate radicals have similar oxidation potentials of 2.60 V compared to 2.70 V ($OH^{\bullet}$ at pH = 3.0).[27] These radical reactants readily attack a variety of chemical bonds of organic molecules, occasionally leading to complete degradation.[18,20,27-29] In addition, the remaining sulfate radicals scavenge electrons from the broken bonds and unused activating agents (Eq. 2) to form unreactive sulfate ions.

$$SO_4^{\bullet-} + Fe^{2+} \rightarrow SO_4^{2-} + Fe^{3+} \quad \text{(Eq. 2)}$$

Despite the benefits that persulfate offers as an ISCO oxidant, persulfate tends to nonselectively react with contaminants in groundwater. As a result, treatment of target contaminants would be difficult as most of the oxidant supply would be prematurely consumed from early persulfate activation/decomposition.[30,31] In addition, groundwater is a flow system. Treatment options such as constant dosing of oxidant would be both laborious and time-consuming. Thus, ISCO treatment of groundwater pollution should be primarily focused on the continuous delivery of oxidant at a desired concentration while accounting for the gradient of groundwater's slow-moving system. Some of persulfate

delivery systems that have already been explored include gravity- or pump-feed vertical/horizontal well injection, recirculation system, and pressurized push technology.[19] As for prolonged release studies, diffusion systems which require multiple applications of coatings onto the reagent's surface or the direct mixing of reagent and matrix have garnered widespread interest.[32-35] For example, a persulfate and paraffin wax diffusion system formed primarily through their mixing has been reported.[32,33,36-40] In addition, concrete blocks carrying persulfate have also been studied.[41,42] Though paraffin wax is considered safe and convenient, a limitation to paraffin wax is that it is an organic and can be oxidized by persulfate free radicals during the diffusion process. This may greatly hinder the ability of persulfate to oxidize targeted contaminants. In our work, a new controlled diffusion system has been designed where persulfate is incorporated into matrices comprised of only inorganic materials for the degradation of TCE as a model organic contaminant. Three silica materials consisting of zeolite, diatom, and silica which are, respectively, porous crystalline, amorphous, and a mixture of both solids, were chosen as the core ingredients as they are environmental-friendly and cheap.[43-50] The target TCE concentration of 15 mg L^{-1} was chosen since it falls in the range of the low contaminated zone according to EPA standards.[51] Ferrous sulfate was used as the activating agent to show that the persulfate released from our pellets were capable of decomposing contaminants. Potassium persulfate was chosen over the more common sodium persulfate as potassium persulfate takes longer to dissolve in solution due to its lesser molar solubility. Sustained release of Fe^{2+} ions was also briefly investigated in a separate study.

The use of the inorganic sol-gel to further prolong the release is also studied. The

inorganic sol-gel used in this work is formed through the crosslinking of silica particles when sodium silicate (Na_2SiO_3), also known as water glass, to form a solid array of silicon dioxide as shown in Eq. 3.[52,53]

$$Na_2SiO_3 + 2H^+ \rightarrow SiO_2\downarrow + H_2O + 2\,Na^+ \qquad \text{(Eq. 3)}$$

Hydrolysis of the water-soluble Na_2SiO_3 begins with the slow addition of dilute acid to form SiO_2 sol-gel solution. As the pH of the very basic (pH = 13) Na_2SiO_3 decreases, formation of white colloidal silica was observed in solution. Once pH of the solution reaches 9-10, instantaneous gelation occurs, rendering the gel unable to use. The progression of the sol-gel reaction is shown in **Figure 1**.

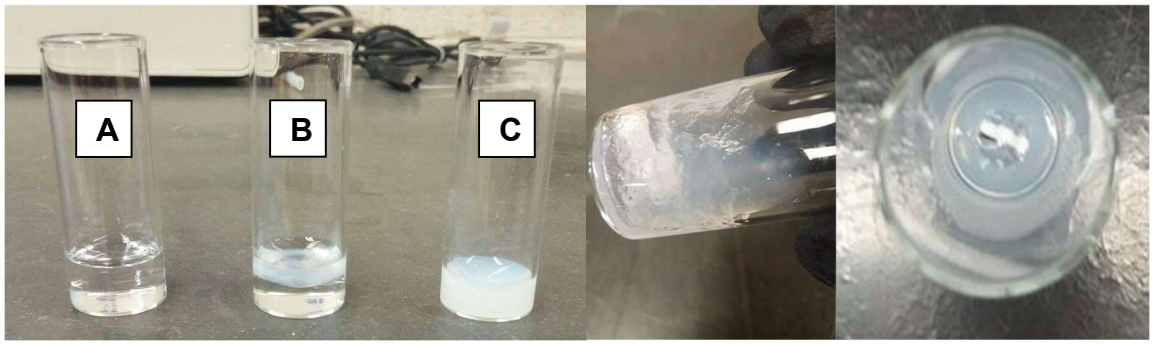


Figure 1. (Left) Sol-gel formation at different pH with gradual lowering of pH (as solution is acidified) from sample **A** to **C**. pH 10 for **C**. (Middle-Right) Additional images of sample **C**.

Since the three matrices selected for our work are either silica- or aluminosilicate-based, the silicate sol-gel would display strong affinity as a binder and coating. In addition, the sol-gel material does not react with either persulfate or Fe^{2+} and is safe for the environment.

Zeolites are naturally occuring crystalline aluminosilicate minerals that possess a wide range of uniform and well-defined pore sizes.[43] Synthetic zeolites have also been produced industrially on a large scale in the form of Types A, beta, mordenite, Y, and ZSM-5 crystals for many applications such as gas adsorption and chemical separation.[43] These manufactured zeolites normally have pore sizes ranging from 3 to 8 Å. Zeolite with pore size of 5 Å (known as 5A zeolite) is inexpensive and one of the most widely used zeolites.[54] Commercial zeolites contain binders, providing the materials with strong structures.[44-46] In the current work, 5A zeolite was used for the proof-of-concept studies. Here, zeolite beads were ground into powders, mixed with the $K_2S_2O_8$ powder, and pressed into pellets. Thus, persulfate most likely diffuses through the voids between the pulverized zeolite particles in the pellets. The pore size of the 5 Å zeolite is slightly larger than the persulfate anion (diameter <5 Å), making it possible for persulfate to also diffuse through the pores of the zeolite.[55] In the current work, whether persulfate diffuses through the voids in the pellets or the pores of the zeolite was not investigated.

Diatomite are off-white sedimentary rocks composed of accumulated, fossilized remains of diatoms, a single-celled aquatic algae.[47,48] Found in marine sediments, diatomite is almost entirely silica. Dried crude ore typically shows 80-90% (sometimes 95%) silica (SiO_2) with alumina (2-4%) and hematite (0.5-2%), which is easily crumbled into a very fine amorphous powder.[47] Diatomite is available commercially and widely

used, including applications as filter media, fillers, and materials for absorption and insulation.[47]

Silica flour is a purified form of raw silica found naturally in silica-rich rocks such as sandstone. These ubiquitous polycrystalline powders can also be prepared through ball milling and various filtration systems into fine particles with no internal pores.[50] Silica flour has been commercially used in a range of consumer products such as a filler for pharmaceutical drugs and various other products. Since silica flour as a matrix material is not porous, the diffusion pathway of persulfate is expected to go between gaps of packed particles instead of through pores. Furthermore, silica flour does not possess binders in contrast with 5Å zeolite powders.

Zeolites, diatomite, silica flour are inert to persulfate which makes them ideal supports for housing persulfate. The inexpensiveness and accessibility of these inorganic materials allows for easy scalability of the system if even longer release time is desired. Persulfate sustain-released from inert inorganic materials serves as a model reagent for other reagents, such as sodium percarbonate and potassium permanganate, for groundwater remediation.[56-60] In this work, we offer a simple, yet effective way to control the release of strong oxidants such as persulfate for the degradation of organic contaminants.

2. Materials and Methods

Zeolite (5 Å, Grade 522, Mallinckrodt), diatomite (Fossil Shell Flour, Perma-Guard), silica (200 mesh, Short Mountain Silica), sodium silicate (41° Baume in aqueous solution, J.T. Baker), sulfuric acid (H_2SO_4, Certified ACS Plus, Fisher), and potassium persulfate ($K_2S_2O_8$, Certified ACS, Fisher) were used for pellet fabrication. Potassium iodide (KI, Alfa Aesar, 99%) and sodium bicarbonate ($NaHCO_3$, Certified ACS, Fisher) were used for the determination of persulfate. Iron(II) ammonium sulfate hexahydrate $(NH_4)_2Fe(SO_4)_2 \cdot 6H_2O$, Merck), hydroxylamine hydrochloride (Alfa Aesar, 99%), sodium acetate (ACS, >99%), glacial acetic acid (Fisher, Certified ACS), and 1,10-phenantroline (Alfa Aesar, 99+%) were used for Fe^{2+} determination. Ferrous sulfate heptahydrate ($FeSO_4 \bullet 7H_2O$, C.P. Baker's Analyzed) was used for persulfate activation. TCE (Acros Organics, 99+% extra pure), 2-bromofluorobenzene (BFB, Acros Organics, 99%), methanol (HPLC grade, Fisher), sodium chloride (NaCl, Certified ACS, Fisher), acetone (Certified ACS, Fisher) and pentane (Certified ACS, Fisher) were used for TCE determination. Silver nitrate and ammonia solution were used to perform quantitative chloride testing. Sodium nitrate ($NaNO_3$, Certified ACS, Fisher) and sodium chloride were used for chloride analysis. Deionized water (DI, 18.1 MΩ-cm) was obtained from a Barnstead™ E-Pure™ Ultrapure Water Purification system. A Carver 3851 Model C press was used for pressing and a KBr evacuable die set (International Crystal Labs) was used for producing pellets. A Chloride Combination Ion-selective Electrode (Cole-Parmer; Item # UX-27504-08) was used for chloride analysis. A Leica S8AP0 microscope was used to take images of the pellets. Pore size and surface area measurements were conducted for a type **4** pellet on the ASAP 2020 Plus instrument (Micromeritics Instrument Corp.) and the ASiQwin™-Automated Gas Sorption system by Quantachrome Instruments.

2.1 *General pellet preparation*

Silica materials were crushed and sieved prior to mixing with $K_2S_2O_8$ or $FeSO_4 \cdot 7H_2O$ powder. The mixture was then transferred into a die and pressed and held for 1 minute under 5-7 tons of pressure on a 12-ton, manual, two-column hydraulic lab press. Upon retrieval, a quality check was performed to ensure no visible surface cracks. The resulting cylindrical pellet was 13 mm in diameter and its thickness varied depending amount of powder loaded and the material. If not used immediately, the pellet was stored in a sealed small vial purged with N_2. From this general procedure, four methods (Methods **A**-**D**) were produced involving the use of sol-gel, no sol-gel, persulfate, and $FeSO_4$ for making pellets.

Method A (persulfate pellet with sol-gel as a binder)

Method **A** was designed to investigate the influence of sol-gel on pellet integrity and persulfate release. For this method, sol-gel was added to the matrix material and potassium persulfate as a binder. A solution of 0.2 M H_2SO_4 (4 mL) was added dropwise to 1.25 g of aqueous sodium silicate solution under constant stirring. After an additional 5 minutes of stirring, an increase in viscosity is observed. Prior to gelation, a mixture of the support material (0.425 g) and potassium persulfate (0.075 g) was added into the viscous solution. To remove excess water, the sol-gel solution was allowed to cure for one hour and then dried in a 40°C oven over 1.5 days. Potassium persulfate's half-life at 40°C is nearly 2 weeks.[61] The semi-solid gel was then ground and pressed into a disk-shaped pellet.

Method B (persulfate pellet with zeolite)

Method **B** was designed to investigate the influence of sol-gel on pellet integrity and persulfate release. The method involves mixing the support material with potassium persulfate without any added sol-gel. Support material (5A zeolite, diatomite or silica flour; 0.425 g) and potassium persulfate (0.075 g) were ground and mixed. For the zeolite support material, an additional sieving step was performed to ensure a fixed particle size range (90-250 mesh) prior to mixing with ground persulfate. The mixture of fine powder was then pressed into a persulfate pellet. Using fabrication Method **B**, only the zeolite-based pellets remained intact when immersed in water. Slight ruptures are often observed on the surfaces of diatom and silica pellets shortly after pressing which causes them to crumble immediately in water. Thus, only the zeolite-based pellets (**Figure 2**) were tested in this study.

Method C (persulfate pellet with diatomite or zeolite)

Method **C** was designed to investigate the influence of applying sol-gel as a coating on the pellet surface rather than mixing into the pellet matrix (as in Method **A**). Pellets were prepared as in Method **B** prior to coating. A solution of 0.4 M H_2SO_4 (4 mL) was added dropwise to 1.25 g of aqueous sodium silicate solution under constant stirring. After the addition of the acid, the solution was allowed to stir for an additional 5 min to give a sol-gel of increased viscosity. Once viscous enough, the sol-gel was ready to be used for immediate spin coating. The spin coating was conducted on a home-made spin coater by a process similar to those reported earlier.[61-64]

Method D (ferrous sulfate pellet with zeolite)

Method **D** involves the mixing of ferrous sulfate and support material without sol-gel application as the sol-gel solution containing O_2 from air could cause the oxidation of Fe^{2+}. Like Method **B**, sieved zeolite was used as it forms a rigid pellet on its own. Zeolite (0.400 g) and $FeSO_4 \cdot 7H_2O$ (0.100 g) were ground and mixed. The mixture was immediately pressed into a pellet and transferred into a vial and flushed with nitrogen gas. The vial was then capped and sealed with parafilm for later use.

2.2 *Preparation of inorganic sol-gel*

Sodium silicate was acidified with dilute sulfuric acid under constant stirring until an increase in viscosity is first observed. At this state, the sol-gel can now be used for coating as gelation will occur shortly after surface application. If mixing of reagent is desired, persulfate and a select silica media are deposited onto the viscous silicate solution and are allowed to stir until gel formation. The sol-gel transition at this point very brief and difficult to control. The resulting cloudy gel is then set aside to cure at room temperature before placing into an oven to dry. The gel is then inspected for moisture and ground once again. The mixed powder is then pressed into a pellet under 5-7 tons of pressure.

2.3 *Studies of the release of persulfate and $FeSO_4$ from their respective pellets*

Pellets, processed from the general procedure, are each submerged into 500 mL of deionized water in an Erlenmeyer flask. The solution is then stirred at 700 rpm (revolutions per minute) with a mini magnetic stir bar. The flask was sealed with paraffin

to reduce evaporation of solution. Periodically, 2-mL aliquots are extracted over a desired period of time. These samples are labeled and frozen immediately at 0 °C for at least a day. These samples are left to thaw at room temperature for 2-3 hours before UV-Vis spectroscopy.

The analysis method performed for persulfate is based on a modified version of the spectroscopic I^-/I_2 method developed by Liang and coworkers.[65] In this method, an aqueous indicator solution consisting of 0.15 M $NaHCO_3$ and 1.0 M KI and a 25 mM $K_2S_2O_8$ stock solution was prepared. The standards used for the analysis covered the concentration range of 5-120 μM. These standards were prepared by adding 2.5 mL of indicator and the necessary amount of $K_2S_2O_8$ stock to 25-mL volumetric flasks. The resulting reddish-yellow solutions were then allowed to equiliberate for approximate 20 minutes before filling up to the mark. In a similar manner, the blank was prepared by adding 1 mL of indicator to 1 mL of $K_2S_2O_8$ stock. After the 20 minutes, the standards were tested for the formation of I_2 at 352 nm in ascending order starting from the blank. Adjustments were performed out of the lab to account for the missing volume during each extraction. Each experiment was performed in triplicates (n = 3) to give error bars.

Iron-phenanthroline method was used for the Fe^{2+} analysis by measuring the absorbance of the iron-phenanthroline complex at 511 nm. For this method, acetate buffer (pH = 5), 20 mg L^{-1} Fe^{2+} stock (dissolved ferrous ammonium sulfate in aqueous solution), 10 g L^{-1} hydroxylamine hydrochloride, and 2 g L^{-1} 1,10-phenanthroline solutions were prepared. Four standard solutions, covering the range of 5 to 15 mg L^{-1}, were prepared by adding 1 mL of 1-10 phenanthroline, 2.5 mL of hydroxylamine, and 5 mL of acetate buffer to a 50-mL volumetric flask containing the appropriate amount of Fe^{2+} before

diluting to the mark.

2.4 *Preparation of TCE solution and extraction of TCE from treated solutions for GC-MS analysis*

To prepare a 15 mg L^{-1} TCE solution, a 250 mL solution of pure DI water was spiked with TCE in a 250-mL French square glass bottle sealed with a rubber septum. To this solution, one persulfate pellet and a single dose (0.5 g) of ferrous sulfate was added with magnetic stirring at 1200 rpm. Periodically, a 10-mL aliquot was extracted and excess methanol (3.0 mL) was added to quench residual persulfate.[66] The samples were then frozen immediately after quenching. **Figure 14** discusses TCE analyses in such acetone-free TCE solution.

In earlier TCE decomposition studies, 100 mg of TCE in 10 mL of acetone was added DI water to give a 10,000 mg L^{-1} TCE solution. It was subsequently diluted with DI water to make 15 mg L^{-1} TCE solution. TCE is known to readily dissolve in acetone. **Figures 10-13** below are results of TCE analyses in the acetone-containing aqueous solutions.

To extract TCE from the defrosted samples, 3 mL of pentane and bromofluorobenzene (BFB) mixture was added to each aliquot. BFB (0.5 mg L^{-1}) was used as an internal standard to account for the volatility of pentane. Following that, 5.0 g of NaCl was added to help separate the organic and aqueous layer. The vial containing the mixture is then sealed with duct tape and placed onto a Burrell Scientific Wrist Action shaker for 15 minutes. The mixture is then left to stand for 5 minutes before the extraction

of the organic layer into vials for further processing. This procedure is also applied to the premade standards and blank.

2.5 *TCE determination*

Gas chromatography mass spectrometry (GC-MS) was used for determining the amount of TCE present throughout the treatment. The method used was based on the EPA method 551.1, commonly used for chlorinated compounds.[67] TCE stock solution (10,000 mg L^{-1}) was prepared in acetone and allowed to equilibirate for 3 hours. From this stock solution, several serial dilutions were performed to produce 6 aqueous calibration standards with concentration ranges from 0 to 5 mg L^{-1}. Methanol was also added to each standard as well as to the blank to include the quenching performed on the test samples.

GC-MS measurements were performed on an Agilent Technologies 7820A Series GC System with a 7693A Autoinjector. A 5977B mass spectrometer detector, equipped with an Agilent HP-5ms Ultra inert column (30.0 m × 0.25 mm i.d. × 0.25 μm film thickness), was used for chemical analysis. Helium was used as the carrier gas with a flow rate of 1.2 mL min^{-1}. Selected-ion monitoring (SIM) mode was used to scan for TCE (130 and 132 m/z) and BFB (174 and 176 m/z). The temperature programming of this GC-MS method starts with a 1-μL sample injection into an initial oven temperature of 27 °C for 4 minutes, ramped up to 61 °C at 5 °C/min and held for 3 minutes before cooling and a quick bakeout up to 300 °C. The estimated limit of detection (3σ) for our TCE method was 0.057 mg L^{-1}.

2.6 *Chloride analysis*

In the chloride analysis after the treatment, chloride standards, which covered a range of 1-50 mg L^{-1} (ppm), were first prepared from a stock solution of 1000 mg L^{-1} Cl^- on the same day of analysis. A single, 30-mL aliquot was taken from a treated TCE solution at the end of the 8-h treatment using one type **1** pellet. To the aliquot, 3 mL of methanol was added as a quenching agent for the remaining reactive $SO_4^{\bullet-}$ and mixed thoroughly. Iron oxide particles free-flowing in the TCE aliquot were removed via suction filtration to avoid interference with the membrane of the electrode used below. From the sample, three 10-mL aliquots were produced. Shortly after, an ionic strength adjusting solution (1.0 M $NaNO_3$, 0.10 mL) was added to each of the 10-mL aliquots containing methanol under constant stirring at 1050 rpm (revolutions per minute). When the Chloride-Combination Ion-selective Electrode (Cole Palmer; Item # UX-27504-08) used for chloride analysis was stabilized, mV readings were recorded. The last 5 stable readings were used for chloride calculations for each sample or standard.

Blank solutions containing 250 mL of deionized water, one type **1** pellet, 0.5 g of $FeSO_4•7H_2O$ were prepared and stirred at 1200 rpm. A 10-mL aliquot was then retrieved and mixed with 1.0 mL of MeOH. Chloride analysis for the MeOH-containing blank solutions was performed by the procedure described above for TCE-treated solutions. The chloride contents from the blank solutions were subtracted from those of the TCE-treated solutions to give the chloride concentrations from the TCE treatment by the persulfate-containing pellet.

2.7 *Characterization of type **4** pellet by the BET method*

Nitrogen adsorption/desorption experiments were conducted using the Brunauer, Emmett, and Teller (BET) method to measure the specific area and porosity of a material.[68] Two different BET measurements were conducted using the ASAP 2020 V4.01 system by Micromeritics Instrument Corp. and the ASiQwin™-Automated Gas Sorption system by Quantachrome Instruments.

For the BET measurement, type **4** pellet was crushed into pieces of varying sizes and ~0.20 g was weighed and transferred to a tube. The tube was then degassed overnight at 50 °C to remove trapped moisture that may have accumulated during the pressing of pellet. After that, N_2 as the adsorbate gas, is introduced to the sample at 77 K. The volume of adsorbed gas was then measured at increasing relative pressure to create a multi-point isotherm.

3. Results and Discussion

3.1 *Methods for pellet fabrication*

Four methods (**A**-**D**) for pellet preparation were developed to provide a variety of treatment options. These options range from pellets with short preparation time and fast chemical release to pellets which required additional procedural steps to achieve much longer duration of release. In addition, Fe^{2+} pellets from Method **D** are available as potential prolonged activation method for control-released persulfate. From the four methods, a total of 6 pellets with nominal masses of 0.5 g and 1.0 g were developed and the key features of each method is summarized in Table **1** below.

As a precursor method, Method **B** was initially applied to each support material as the process required short preparation time, approximately 10-15 minutes per pellet. Upon immersion of the pellets into solution, fracturing was observed for both silica and diatom pellets. Consequently, rapid release of persulfate occurred within a 2-h period at most. Only the zeolite pellets which were designated as type **4** pellet (**Figure 2**), remained whole. As mentioned earlier, the 5A zeolite possessed aluminum-based binders, unlike the other two materials, which helped maintain the pellet's structural integrity. As a result, the inorganic sol-gel approach was considered, and Method **A** was developed. In addition, Method **C** was applied to see if extra coating layers would further increase the duration of persulfate release. A comparison image of the uncoated and coated pellets is shown in **Figure 3**.

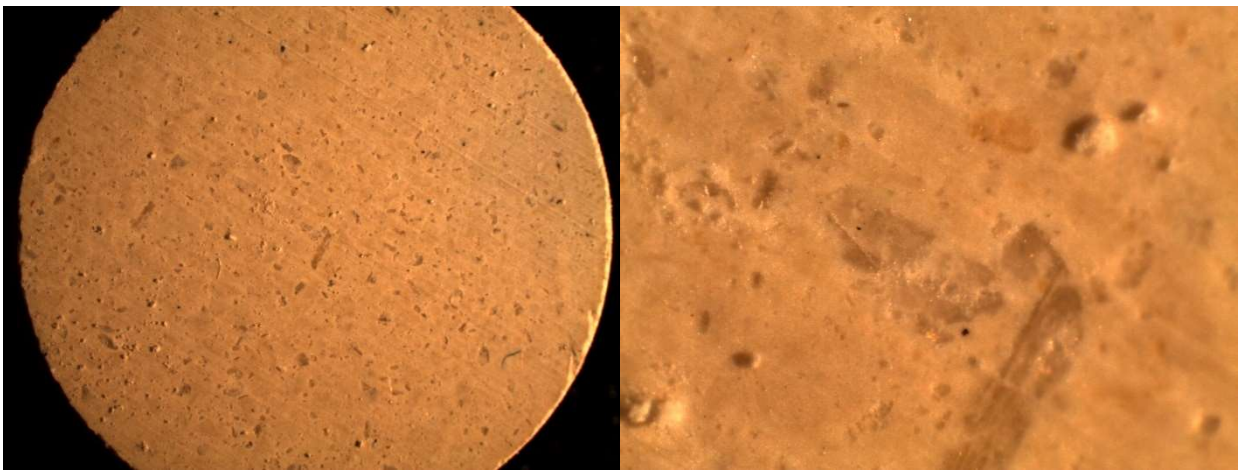


Figure 2. Image of Method **B** persulfate-zeolite pellet (left), surface image of same pellet with 10x magnification (right).

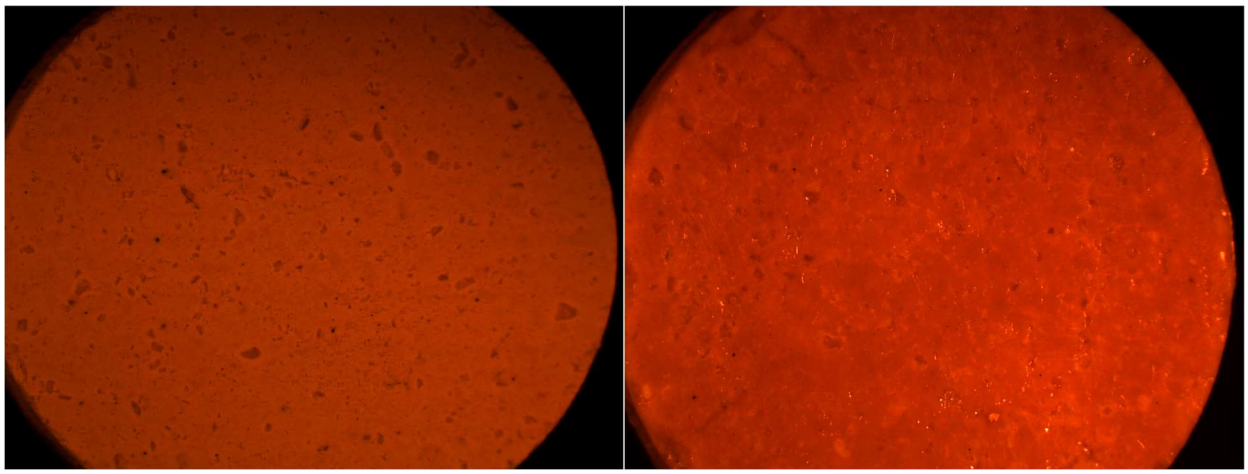


Figure 3. Images of pellets by **Method B** (Left) vs. by **Method C** (Right). These were persulfate-zeolite pellets with a thin layer of sol-gel coating for the pellet on the right.

Table 1. Key features and pellets of **Methods A-D**

Methods	Key features	Pellet type	Chemical	Matrix material	Weight[1] (g) & Thickness[2] (mm)
A	Sol-gel uniformly mixed with matrix material and persulfate prior to forming pellet; Sol-gel acts as a binder between support and persulfate	**1**	$K_2S_2O_8$	zeolite	1.2 g/6.0 mm
		2	$K_2S_2O_8$	diatom	1.1 g/5.3 mm
		3	$K_2S_2O_8$	silica	1.0 g/4.3 mm
B	Matrix material mixed with persulfate without sol-gel application	**4**	$K_2S_2O_8$	zeolite	0.5 g/2.6 mm
C	Sol-gel applied as a surface coating on pellet	**5**	$K_2S_2O_8$	zeolite	0.5 g/2.7 mm
D	Uniform mixture of matrix and ferrous sulfate pressed into pellet; no sol-gel involved	**6**	$FeSO_4$	zeolite	0.5 g/2.6 mm

[1] Average of 3 pellets.

[2] Diameter for all pellets is 13 mm.

3.2 *Diffusion studies of pellets*

Types **1**-**5** pellets were tested in DI water to study the release of persulfate through different matrix materials and with and without the involvment of sol-gel. Upon submerging the pellet into solution, the bottom face of the pellet is in contact with glassware, thereby obstruction diffusion from that side. As a result, diffusion through the surface and sides of the pellet is most probable.

3.2.1 *Zeolite-based pellets*

The diffusion of types **1**, **4**, and **5** pellets were studied upon immersion of the pellets into DI water. The averaged (n = 3) diffusion profiles of these pellets are reported below. The maximum range for time was cut short based on where the percent release seemed to first plateau.

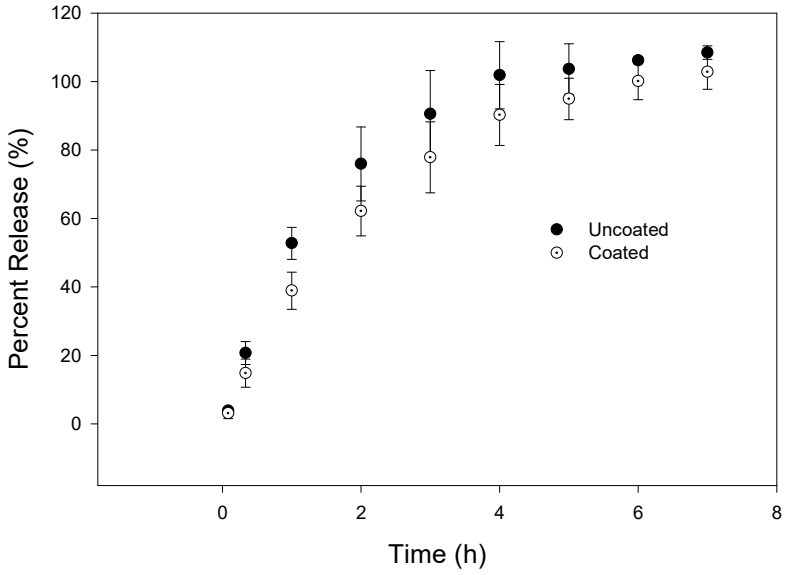


Figure 4. Persulfate release profiles of types **4** (uncoated) and **5** pellets (coated). Error bars were used to represent the results of 3 pellets.

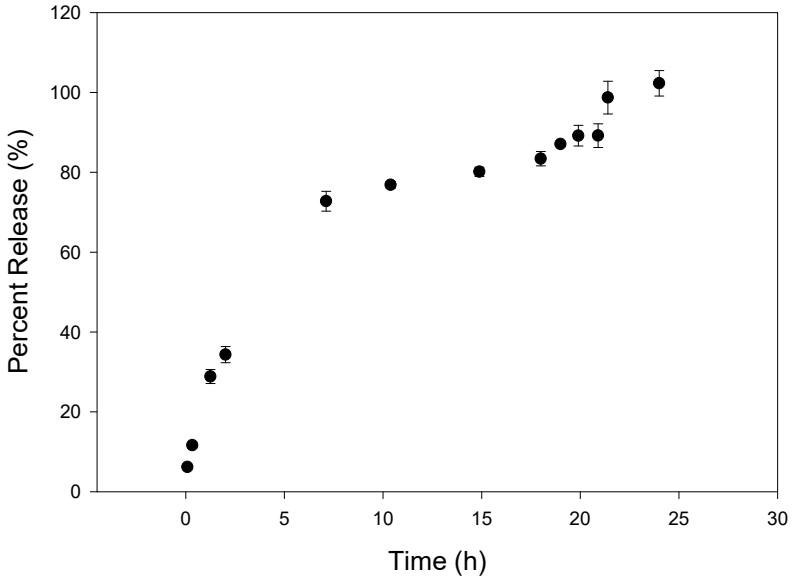


Figure 5. Persulfate release profile of type **1** pellet (zeolite). Error bars were used to represent the results of 3 pellets.

According to **Figure 4**, there seems to be a 10% slower diffusion for the coated type **5** pellet as compared to uncoated type **4** pellet . This showed that the extra spin-coated layer helped increase the duration of chemical release. Approximately 50% persulfate is released within the first hour followed by a slow release until maximum persulfate release was achieved at the 7-hour mark. During the mixing of the matrix and persulfate, the persulfate particles located on the outsides of the pellet may be responsible for the fast initial release as they immediately dissolve in solution when immersed. Though the sol-gel spin coating represented by Method **C** was considered effective, the process required meticulous steps to prepare the sol-gel, thereby reducing the effeciency of our studies in the limited time available. As a result, it was only applied to zeolite-based type **4** pellet and not to diatom and silica flour pellets.

The diffusion profile of type **1** pellet in **Figure 5** showed a complete persulfate release at approximately 24 hours in consequence to the addition of sol-gel as represented by Method **A**. Compared to its precursor type **4** pellet, there was more than a threefold increase in release time.

3.2.2 *Diatomite-based pellets*

Diatom pellets created with Method **B** in previous works were unable to hold in solution causing all the persulfate to release instantly. As a result, only Method **A** which also uses sol-gel as a binder was applied. The diffusion profile of the resulting type **2** pellet is shown in **Figure 6**.

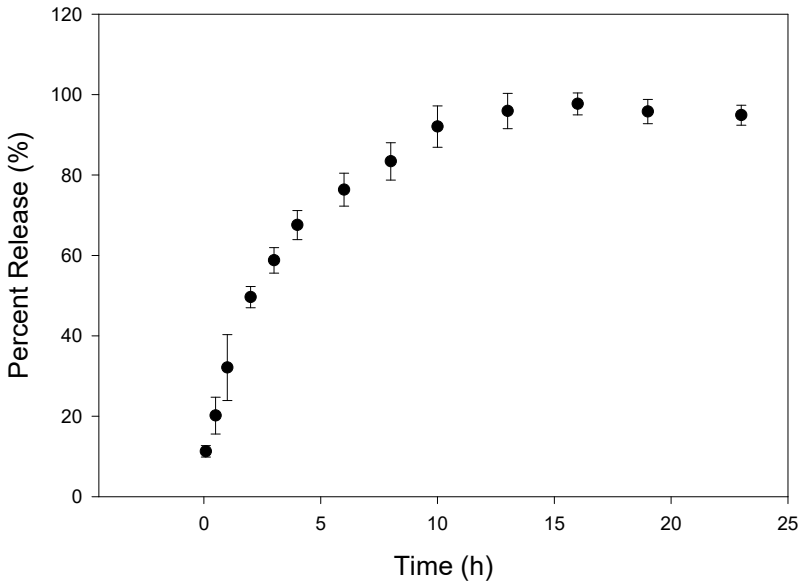


Figure 6. Persulfate release profile of type **2** pellet (diatomite). Error bars were used to represent 3 pellets.

A maximum persulfate release of 97% is observed at the 16-hour mark. Similar to previous pellets, a rapid release of 50% occurs in the first two hours.

3.2.3 *Silica flour-based pellets*

Like diatom, binderless silica flour pellets also did not hold together in solution and so Method **A** was applied. The diffusion profile for these pellets were measured and shown in **Figure 7**.

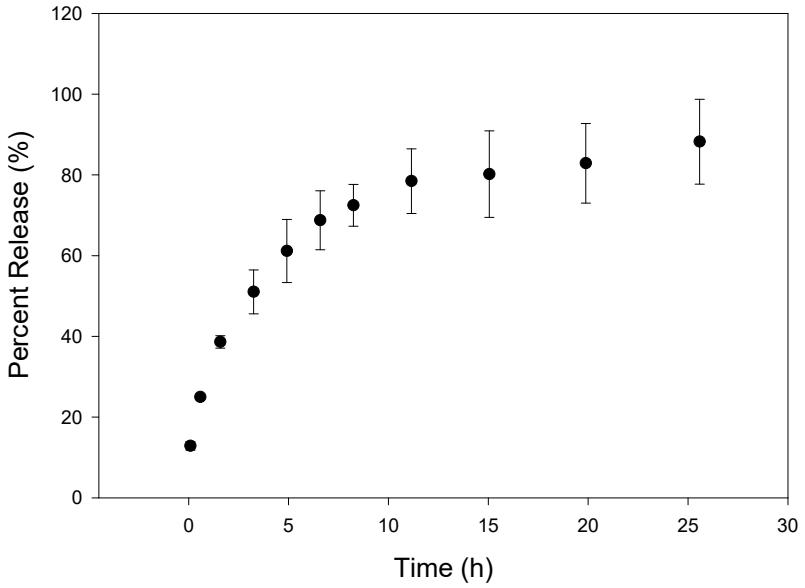


Figure 7. Persulfate release profile of type **3** pellet (silica flour). Error bars were used to represent results of 3 pellets.

Up to 90% persulfate release is shown for type **3** pellet within a 25-hour period. Once again, fast persulfate release is observed within the first few hours. Compared to the other pellets, it seems that type **3** pellet had the longest release time.

3.3 *Fe^{2+} release profile*

Ferrous sulfate pellets (20% w/w; **Figure 8**) with nominal masses of 0.5 g were made in a similar way as Method **B** using zeolite as the support matrix. The Fe^{2+} release from these pellets were characterized as shown in **Figure 9**.



Figure 8. Image of a type **6** pellet containing ferrous sulfate.

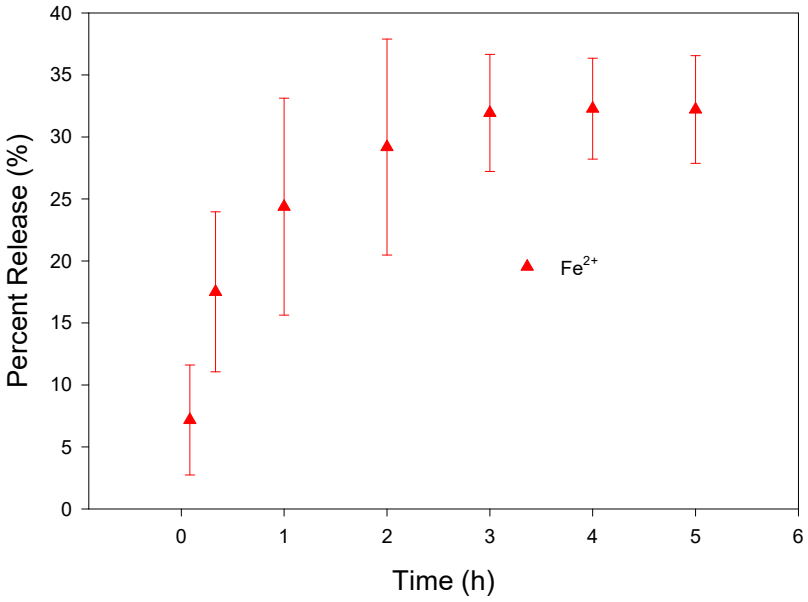


Figure 9. Fe^{2+} release profile of type **6** pellets. Error bars were used to represent results of 3 pellets.

A maximum of 33% Fe^{2+} release was measured within the first three hours of release time from type **6** pellet. The significantly low amount may be attributed to the affinity of the silica material to Fe^{2+} ions, causing most of the latter to be trapped inside or on the surfaces of the pellet. Though this is the probable case, the remaining Fe^{2+} ions on the pellets may still used for persulfate activation, as dissolved persulfate ions can diffuse into the pellet. After the the Fe^{2+} ions trapped in the type **6** pellets were used the activate persulfate in solution, the pellets crumbled into smaller pieces. In comparision, the persulfate pellets remained essentially intact after the persulfate release.

3.4 *Control-released persulfate for TCE treatment studies*

Simulation for treating TCE-spiked solutions were carried out in batch experiments. For each experiment, a persulfate pellet with single dose of Fe^{2+} were used to treat 15 mg L^{-1} TCE. Based off the diffusion profiles shown earlier, optimized type **1-3** pellets made from Method **A** and type **4** pellet from Method **B** were chosen for these studies. Three experiments were conducted separately at different times to account for deviation. The degradation plots are shown in **Figures 10-14** below. Each data point represents the three separate experiments (conducted at different times). However, GC-MS analyses of TCE concentrations in the three samples from the separate runs were conducted at the same time. We speculate that a random error during the GC-MS analysis of the three samples may be responsible for the sudden dip in TCE concentration at the 2-hour point in **Figure 13**.

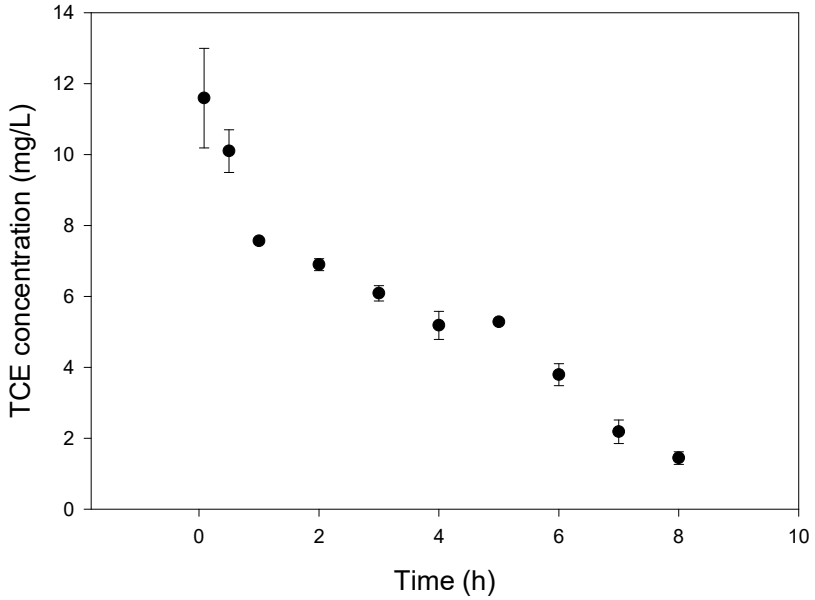


Figure 10. Degradation of TCE in acetone-containing solution with type **1** pellet (zeolite). Error bars were used to represent results of 3 separate runs.

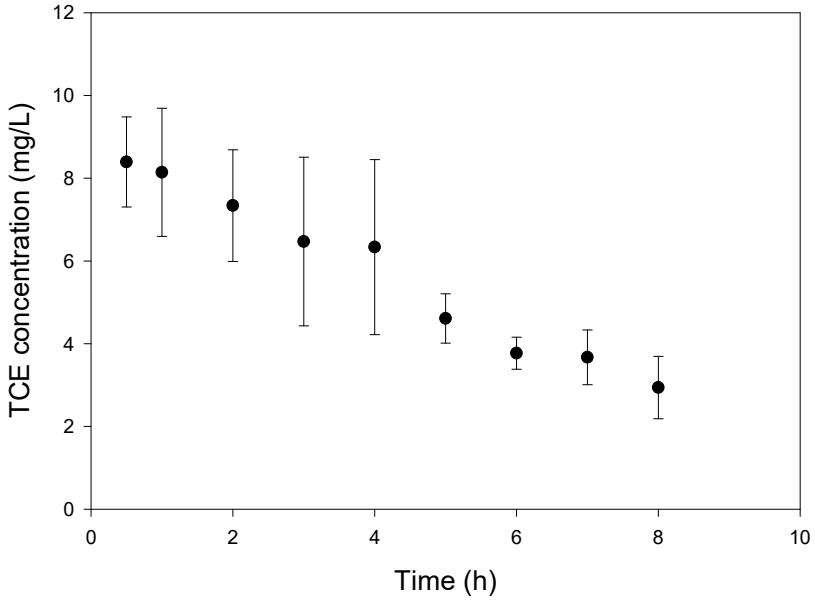


Figure 11. Degradation of TCE in acetone-containing solution with type **2** pellet (diatom). Error bars were used to represent results of 3 separate runs.

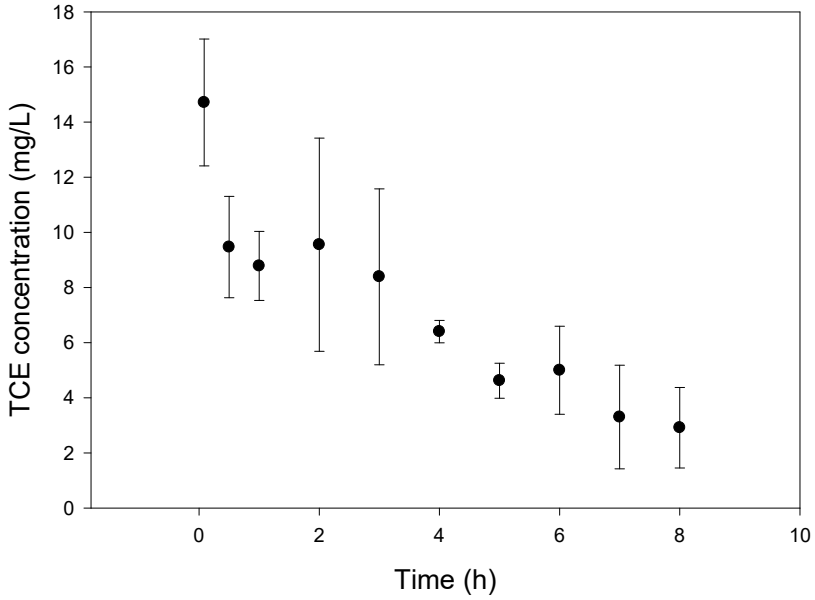


Figure 12. Degradation of TCE in acetone-containing solution with type **3** pellet (silica flour). Error bars were used to represent results of 3 separate runs.

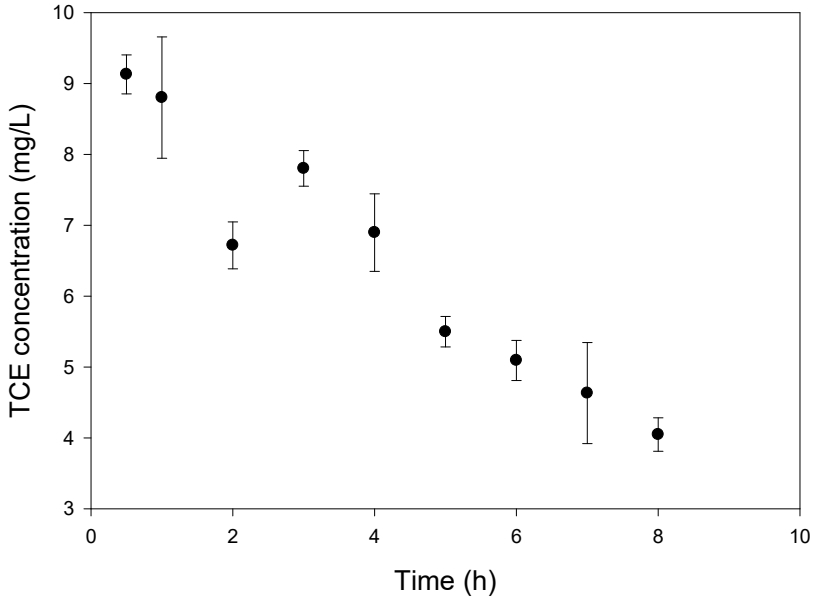
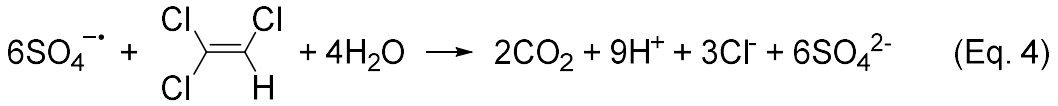


Figure 13. Degradation of TCE in acetone-containing solution with type **4** pellet (zeolite/no sol gel). Error bars were used to represent results of 3 separate runs. Possible reason for the dip in TCE concentration at the 2-hour point is given on p. 29.

After 8 hours of treatment, there were 1.44 ± 0.12 mg L^{-1}, 2.94 ± 0.53 mg L^{-1}, 2.91 ± 1.46 mg L^{-1}, and 4.04 ± 0.25 mg L^{-1} TCE leftover of what was originally 15 mg L^{-1} TCE solution for type **1-4** pellets, respectively. In other words, 73.0-90.4% of TCE was degraded. In addition, approximately 50% of the TCE is rapidly decomposed after the first 30 minutes of treatment. Within this brief period of time, single dose Fe^{2+} is quickly used up to activate persulfate, suggesting that most of the Fe^{2+} was converted to inactive Fe^{3+} in the first hour.

Since acetone was used in an earlier step to help dissolve TCE in solution, concentrations of lower than 1 mg L^{-1} TCE was not achieved. In addition, the concentrations of acetone were not measured. As a result, separate experiments using only type **1** pellet were performed without the use of acetone during the preparation of aqueous TCE solution. The TCE solution was left capped overnight under constant stirring to ensure that TCE was fully dissolved. Treatment studies were performed once more as described previously and the results are shown in **Figure 14**.

During TCE treatment, a pH test was performed on the treated solution, showing a pH drop from 9 to 3 within the first 30 minutes. This sharp decline may be attributed to the production of hydrochloric acid and sulfuric acid from degradation of TCE, as shown in **Eq. 4**. In the reaction in **Eq. 4**, C and H atoms in TCE are oxidized by sulfate radicals into CO_2 and H^+ ion, respectively.



(Eq. 4)

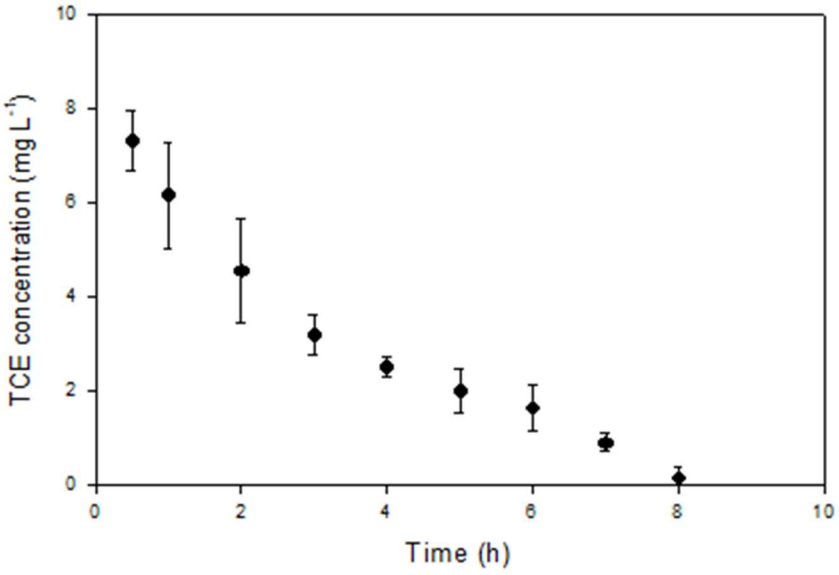


Figure 14. Degradation profile of TCE in acetone-free solution with type **1** pellet (zeolite). Error bars were used to represent results of 3 separate runs.

After 8 hours, TCE concentration ranged from under the detection limit (<0.057 mg L^{-1}) to barely detectable levels of 0.16 ± 0.16 mg L^{-1}. This indicates that acetone previously used in the studies may have interfered with the oxidation process as acetone is organic.

3.5 *Results of chloride analysis*

TCE can release up to three chloride ions per molecule during decomposition. Chloride analysis was performed to help correlate the degradation of TCE reported through GC-MS to the formation of chloride in solution. For this study, only TCE solutions treated by type **1** pellet were analyzed for chloride.

Chloride analysis showed that there were 10.8 ± 0.4 mg L^{-1} Cl^- ions in the TCE solution treated by type **1** pellet. Theoretically, if full dehalogenation occurs for a 15 mg

L^{-1} TCE solution, the expected Cl^- concentration in the treated solution would be 12.0 ± 0.7 mg L^{-1}. Though the values do not match up perfectly, up to 90% of the chloride was detected. This suggests that partial dehalogenation of TCE had occurred throughout treatment. Chloride byproducts or TCE daughter products were not quantified to further prove this theory.

3.6 *Studies of pore size distribution*

Multi-point measurements were performed solely on type **4** pellet with two different BET instruments. As the only dry pellet, the risk of introducing excess moisture to the machine is greatly reduced as the outgassing process would not have been sufficient enough. The following, including Figures 15-17, is a description of the measurement by the Micrometrics ASAP 2020 V4.01 system. The specific surface area and average pore diameter below are the averages of the two different BET measurements.

A 49-point isotherm was produced and is given in **Figure 15**. From the isotherm, data within the range of 0.05 and 0.35 relative pressure were used to calculate the BET surface area plot in **Figure 16**. In addition, pore size distribution was determined, as shown in **Figure 17**.

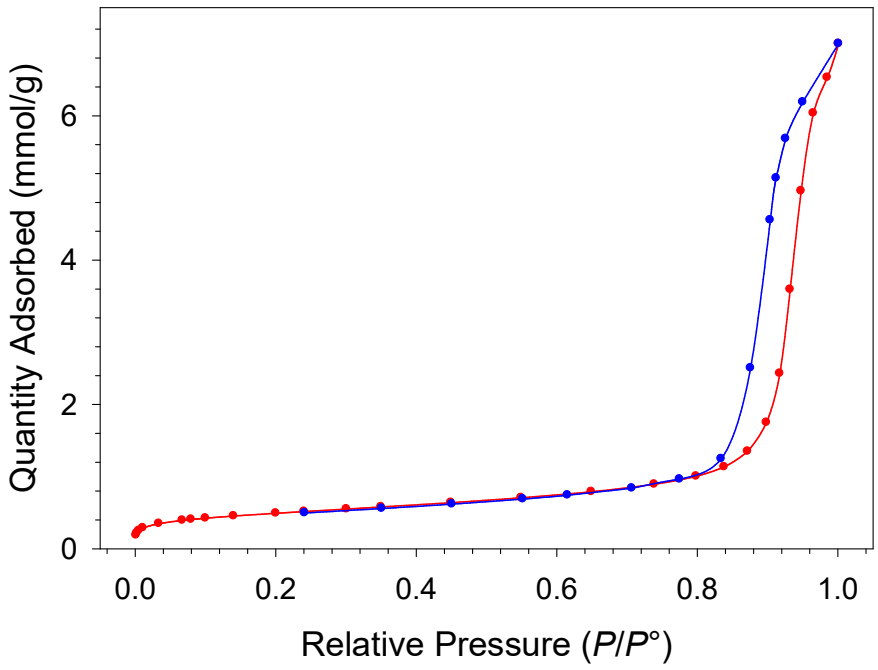


Figure 15. Nitrogen adsorption/desorption isotherm of a type **4** pellet.

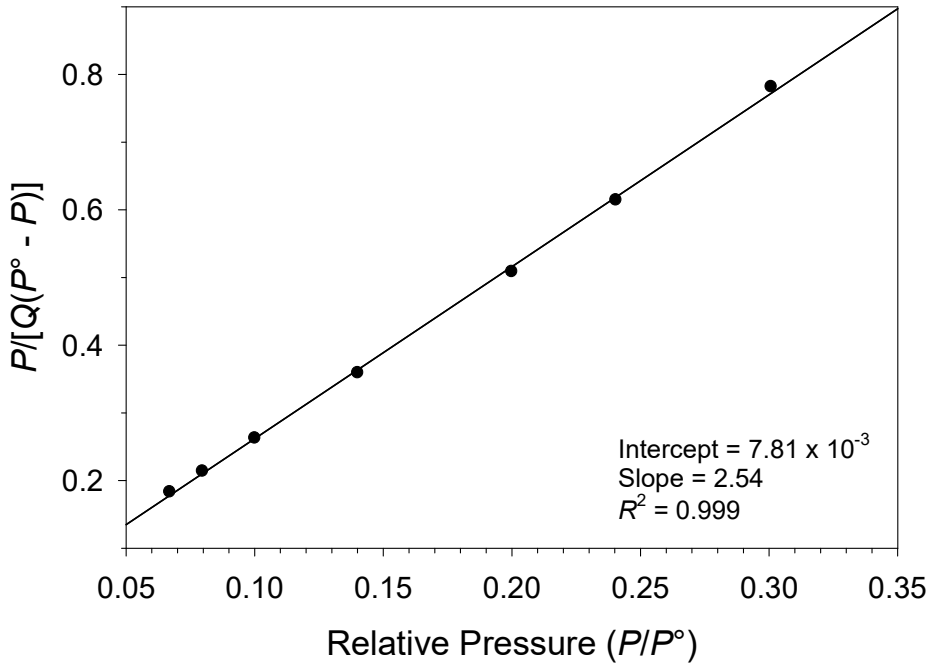


Figure 16. BET surface area plot of a type **4** pellet. *Q* = quantity of N_2 adsorbed (mmol/g).

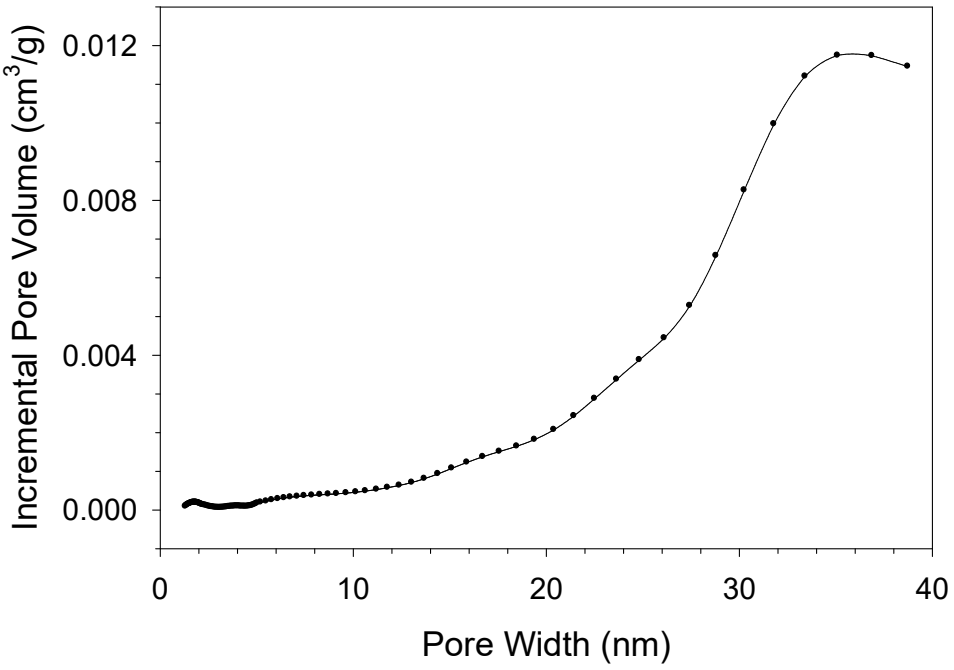


Figure 17. Incremental pore volume vs. pore width plot demonstrating the size distribution for the type **4** pellet.

Using the BET surface area plot, the average specific surface area of zeolited-based type **4** pellet was 36.5 ± 1.8 m^2/g. As for pore size distribution, type **4** pellet is considered to be mesoporous as majority of its pore sizes were ~34 nm with a pore size average of 23.6 ± 0.1 nm. These large pore sizes were likely generated during the grinding process of 5A zeolite sieves into fine powder. When pressed together with persulfate, formation of voids within the pellet are likely to occur. Though this is the case, successful persulfate release and treatment of TCE has been proven. Furthermore, the low surface area which resulted from pressing, helped with the slow release of persulfate.

3.7 *Preliminary studies of TCE treatments by released persulfate and Fe^{2+} ions from their respective pellets*

Type **6** pellet was used to activate persulfate for TCE treatment. In this study, a single $FeSO_4 \cdot 7H_2O$ (20% w/w) pellet (type **6**) and one type **4** pellet were used to treat a 15 mg L^{-1} TCE solution. After 6 hours of treatment, TCE concentrations as low as 1.0 mg L^{-1} were detected. This indicates that treatment of TCE with the control-released Fe^{2+} pellets was comparable if not better than the single dose method. However, further experimentation is necessary to prove this as only a single run was performed and the control-released method for Fe^{2+} is still unoptimized.

A separate qualitative study was performed to treat 13 mg L^{-1} of TCE spiked into a Tennessee river water sample to see if treatment of TCE was possible with DOM present. Prior to treatment, an aliquot of the sample was tested under slightly acidic conditions with silver nitrate to negligible levels of chloride ions. After that, a single type **4** pellet and type **6** pellet were added simultaneously to each TCE-spiked solution and the treatment process was monitored as shown in **Figure 18.**

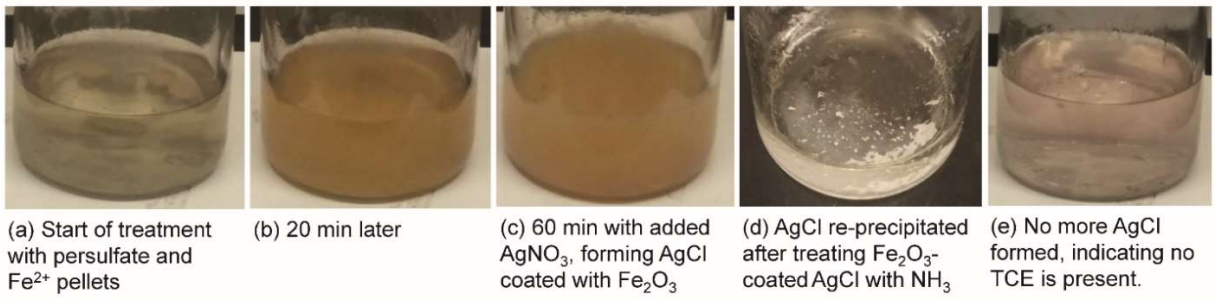


Figure 18. Photos of the treatment process of a river water sample spiked with TCE, followed by silver chloride test.

Formation of cloudy orange residue was observed in the first 20 minutes of treatment (**Figure 18b**). Once treated for one hour, silver nitrate was added to the TCE solution to form silver chloride with Cl^- ions from the decomposed TCE coated with insoluble Fe_2O_3 (**Figure 18c**). Since the solution was already acidic, addition of dilute nitric acid was not needed. Ammonia was then added to form soluble $Ag[(NH_3)_2]^+$ ions and the resulting solution was filtered to remove Fe_2O_3. The silver chloride was then reprecipitated by acidifying the solution (**Figure 18d**) and the solution was filtered to remove AgCl.

We subsequently conducted the following tests to confirm that the decomposition of TCE in the spiked river water, as described in the previous two paragraphs, was complete. One type **4** and **6** pellet each were added to the filtered solution. After one hour, the silver chloride test was performed once again, showing no more sign of AgCl formation (**Figure 18e**). These tests indicated that, after the initial treatment (and AgCl removal described in the previous paragraphs), the TCE level in the solution was below the level that the AgCl test could detect. In other words, the amount (or concentration) of Cl^- ions, generated from the TCE decomposition by $K_2S_2O_8$ and $FeSO_4$ from the newly added type **4** and **6** pellets, was too low to be detected by the silver chloride test.

4. Conclusion

Four methods (**A-D**) involving solely inorganic materials to make persulfate and Fe^{2+} pellets were developed and characterized for the treatment of organic contaminants. One major unique feature of the pellets in this study, in comparison to organic matrix-based controlled release systems such as paraffin wax, is that the inorganic matrices here do not react with the persulfate reagent. In addition, zeolite, diatom, silica flour, and silica gel are all inert, cheap, and naturally abundant.

In this work, control-released persulfate from our pellets with single dose Fe^{2+} or Fe^{2+} pellets, proved successful in treating 15 mg L^{-1} TCE. A degradation of up to 99+% TCE was reported after 8 hours of treatment by type **1** pellet and a single dose of Fe^{2+} ions. Furthermore, the highest release time of persulfate achieved was 25 hours for type **3** pellet when sol-gel was incorporated into the pellet. This does come at a cost for longer preparation time as type **4** pellet which involves no sol-gel application and is limited to zeolite, requires much shorter time to produce. Given the small size of these pellets, they serve as a proof of concept that with further research and expansion, even longer release time can be attained if desired. *Larger pellets (than the current ones with 13 mm diameter, ~3-6 mm in thickness, and 0.5-1.2 g) are expected to lead to longer release.* Sustained release of other reagents, such as sodium percarbonate and potassium permanganate, may be similarly conducted.[56-60]

Since single dose of Fe^{2+} ions was mainly used for our treatment studies, the rapid conversion of Fe^{2+} to Fe^{3+} still remains a problem. Further studies will need to be conducted to improve the Fe^{2+} pellets' release time though we believe that the unreleased (~67%) Fe^{2+} ions within the pellet is still effective at activating persulfate. In addition, the degradation may be improved by introducing a system with sustained addition or release

of Fe^{2+} ions with a chelating agent. Ideally, both persulfate and Fe^{2+} ions will both be control-released within a prolonged period of time, simultaneously. Overall, we believe that these pellets can be used to house a variety of strong oxidants for groundwater remediation of organic contaminants.

References

1. EPA, U. S., *Remediation Technologies for Cleaning up Contaminated Sites (https://www.epa.gov/remedytech/remediation-technologies-cleaning-contaminated-sites)*. 2017.
2. Stroo, H. F.; Leeson, A.; Marqusee, J. A.; Johnson, P. C.; Ward, C. H.; Kavanaugh, M. C.; Sale, T. C.; Newell, C. J.; Pennell, K. D.; Lebron, C. A.; Unger, M., Chlorinated Ethene Source Remediation: Lessons Learned. *Environ Sci Technol* **2012,** *46*, 6438-6447.
3. Stroo, H. F.; Unger, M.; Ward, C. H.; Kavanaugh, M. C.; Vogel, C.; Leeson, A.; Marqusee, J. A.; Smith, B. P., Remediating chlorinated solvent source zones. *Environ Sci Technol* **2003,** *37*, 224a-230a.
4. Hayman, M.; Dupont, R. R., *Groundwater and Soil Remediation: Process Design and Cost Estimating of Proven Technologies*. ASCE Press: Reston, Virginia, 2001.
5. EPA, U. S., *Dense Nonaqueous Phase Liquids (DNAPLs; https://clu-in.org/contaminantfocus/default.focus/sec/Dense_Nonaqueous_Phase_Liquids_(DNAPLs)/cat/Overview/)*. 2017.
6. Wanner, P.; Parker, B. L.; Chapman, S. W.; Aravena, R.; Hunkeler, D., Quantification of Degradation of Chlorinated Hydrocarbons in Saturated Low Permeability Sediments Using Compound-Specific Isotope Analysis. *Environ Sci Technol* **2016,** *50*, 5622-5630.

7. Kirtland, B. C.; Aelion, C. M.; Stone, P. A.; Hunkeler, D., Isotopic and Geochemical Assessment of in Situ Biodegradation of Chlorinated Hydrocarbons. *Environ Sci Technol* **2003,** *37*, 4205-4212.

8. Hunkeler, D.; Aravena, R.; Parker, B. L.; Cherry, J. A.; Diao, X., Monitoring Oxidation of Chlorinated Ethenes by Permanganate in Groundwater Using Stable Isotopes: Laboratory and Field Studies. *Environ Sci Technol* **2003,** *37*, 798-804.

9. Teel, A. L.; Elloy, F. C.; Watts, R. J., Persulfate Activation during Exertion of Total Oxidant Demand. *Chemosphere* **2016,** *158*, 184-192.

10. Dong, H.; He, Q.; Zeng, G.; Tang, L.; Zhang, L.; Xie, Y.; Zeng, Y.; Zhao, F., Degradation of Trichloroethene by Nanoscale Zero-valent Iron (nZVI) and nZVI Activated Persulfate in the Absence and Presence of EDTA. *Chem. Eng. J.* **2017,** *316*, 410-418.

11. Lin, Y.-T.; Liang, C.; Yu, C.-W., Trichloroethylene Degradation by Various Forms of Iron Activated Persulfate Oxidation with or without the Assistance of Ascorbic Acid. *Ind. Eng. Chem. Res.* **2016,** *55*, 2302-2308.

12. Yan, N.; Liu, F.; Xue, Q.; Brusseau, M. L.; Liu, Y.; Wang, J., Degradation of Trichloroethene by Siderite-catalyzed Hydrogen Peroxide and Persulfate: Investigation of Reaction Mechanisms and Degradation Products. *Chem. Eng. J.* **2015,** *274*, 61-68.

13. Doherty, R. E., The Manufacture, Use, and Supply of Chlorinated Solvents in the United States during World War II. *Environ. Forensics* **2012,** *13*, 7-26.

14. Gilbert, K. M.; Reisfeld, B.; Zurlinden, T. J.; Kreps, M. N.; Erickson, S. W.; Blossom, S. J., Modeling Toxicodynamic Effects of Trichloroethylene on Liver in

Mouse Model of Autoimmune Hepatitis. *Toxicol. Appl. Pharmacol.* **2014,** *279*, 284-293.

15. Swaim, P. D.; Morgan, R.; Mueller, P.; Vorissis, M.; Erdal, U.; Carter, W., Implementing an Effective UV Advanced Oxidation Process. *Proc. Water Environ. Fed.* **2009,** *2009*, 678-688.
16. Garrido-Ramírez, E. G.; Theng, B. K. G.; Mora, M. L., Clays and Oxide Minerals as Catalysts and Nanocatalysts in Fenton-like Reactions — A Review. *Appl. Clay Sci.* **2010,** *47*, 182-192.
17. Huling, S. G.; Pivetz, B. E., *In-Situ Chemical Oxidation (https://archive.epa.gov/ada/web/pdf/insituchemicaloxidation_engineering_issue.pdf), U.S. EPA, Engineering Issue of EPA*. 2006.
18. Tsitonaki, A.; Petri, B.; Crimi, M.; MosbÆK, H.; Siegrist, R. L.; Bjerg, P. L., In Situ Chemical Oxidation of Contaminated Soil and Groundwater Using Persulfate: A Review. *Crit. Rev. Environ. Sci. Technol.* **2010,** *40*, 55-91.
19. Siegrist, R. L.; Crimin, M.; Simpkin, T. J., *In Situ Chemical Oxidation for Groundwater Remediation*. Springer: New York, 2011.
20. Matzek, L. W.; Carter, K. E., Activated Persulfate for Organic Chemical Degradation: A Review. *Chemosphere* **2016,** *151*, 178-188.
21. Liang, C. J.; Bruell, C. J.; Marley, M. C.; Sperry, K. L., Thermally Activated Persulfate Oxidation of Trichloroethylene (TCE) and 1,1,1-Trichloroethane (TCA) in Aqueous Systems and Soil Slurries. *Soil Sediment Contam.* **2003,** *12*, 207-228.

22. Liang, C.; Bruell, C. J.; Marley, M. C.; Sperry, K. L., Persulfate oxidation for in situ remediation of TCE. II. Activated by chelated ferrous ion. *Chemosphere* **2004,** *55*, 1225-1233.

23. Kolthoff, I. M.; Miller, I. K., The Chemistry of Persulfate. I. The Kinetics and Mechanism of the Decomposition of the Persulfate Ion in Aqueous Medium1. *J. Am. Chem. Soc.* **1951,** *73*, 3055-3059.

24. House, D. A., Kinetics and Mechanism of Oxidations by Peroxydisulfate. *Chem. Rev.* **1962,** *62*, 185-203.

25. Cashman, M. A.; Kirschenbaum, L.; Holowachuk, J.; Boving, T. B., Identification of hydroxyl and sulfate free radicals involved in the reaction of 1,4-dioxane with peroxone activated persulfate oxidant. *J. Hazard. Mater.* **2019,** *380*, 120875.

26. Eberle, D.; Ball, R.; Boving, T. B., Peroxone activated persulfate treatment of 1,4-dioxane in the presence of chlorinated solvent co-contaminants. *Chemosphere* **2016,** *144*, 728-735.

27. Zhang, B.-T.; Zhang, Y.; Teng, Y.; Fan, M., Sulfate Radical and Its Application in Decontamination Technologies. *Crit. Rev. Environ. Sci. Technol.* **2015,** *45*, 1756-1800.

28. Liu, H.; Bruton, T. A.; Doyle, F. M.; Sedlak, D. L., In Situ Chemical Oxidation of Contaminated Groundwater by Persulfate: Decomposition by Fe(III)- and Mn(IV)-Containing Oxides and Aquifer Materials. *Environ Sci Technol* **2014,** *48*, 10330-10336.

29. Eberson, L., Electron-Transfer Reactions in Organic Chemistry. In *Advances in Physical Organic Chemistry Volume 18*, 1982; pp 79-185.

30. Sra, K. S.; Thomson, N. R.; Barker, J. F., Persistence of Persulfate in Uncontaminated Aquifer Materials. *Environ Sci Technol* **2010,** *44*, 3098-3104.

31. Sra, K. S.; Whitney, J. J.; Thomson, N. R.; Barker, J. F. In *Persulfate Decomposition Kinetics in the Presence of Aquifer Materials*, Proceedings of the Annual International Conference on Soils, Sediments, Water and Energy, 2007; Article 29, pp. 291-299.

32. Kambhu, A.; Comfort, S.; Chokejaroenrat, C.; Sakulthaew, C., Developing Slow-release Persulfate Candles to Treat BTEX Contaminated Groundwater. *Chemosphere* **2012,** *89*, 656-664.

33. Liang, C.; Chen, C.-Y., Characterization of a Sodium Persulfate Sustained Release Rod for in Situ Chemical Oxidation Groundwater Remediation. *Ind. Eng. Chem. Res.* **2017,** *56*, 5271-5276.

34. Wang, L.; Liu, X., Sustained release technology and its application in environmental remediation: A review. *Int. J. Environ. Res. Public Health* **2019,** *16*.

35. Langer, R., New Methods of Drug Delivery. *Science* **1990,** *249*, 1527-1533.

36. Chokejaroenrat, C.; Sakulthaew, C.; Satapanajaru, T.; Tikhamram, T.; Pho-Ong, A.; Mulseesuk, T., Treating Methyl Orange in a Two-Dimensional Flow Tank by In Situ Chemical Oxidation Using Slow-Release Persulfate Activated with Zero-Valent Iron. *Environ. Eng. Sci.* **2015,** *32*, 1007-1015.

37. Dhananjeyan, M. R.; Fine, E.; Kiwi, J., Synthetic Polymer Delivery System: Sustained Release of Persulfate during the Photo-oxidation of an Azo-dye. *J. Photochem. Photobiol. A* **2000,** *136*, 125-131.

38. Christenson, M. D.; Kambhu, A.; Comfort, S. D., Using slow-release permanganate candles to remove TCE from a low permeable aquifer at a former landfill. *Chemosphere* **2012,** *89*, 680-687.

39. Christenson, M.; Kambhu, A.; Reece, J.; Comfort, S.; Brunner, L., A five-year performance review of field-scale, slow-release permanganate candles with recommendations for second-generation improvements. *Chemosphere* **2016,** *150*, 239-247.

40. Kang, N.; Hua, I.; Rao, P. S. C., Production and Characterization of Encapsulated Potassium Permanganate for Sustained Release as an in Situ Oxidant. *Ind. Eng. Chem. Res.* **2004,** *43*, 5187-5193.

41. Liang, S. H.; Kao, C. M.; Kuo, Y. C.; Chen, K. F., Application of persulfate-releasing barrier to remediate MTBE and benzene contaminated groundwater. *J. Hazard. Mater.* **2011,** *185*, 1162-1168.

42. Liang, S. H.; Kao, C. M.; Kuo, Y. C.; Chen, K. F.; Yang, B. M., In situ oxidation of petroleum-hydrocarbon contaminated groundwater using passive ISCO system. *Water Res.* **2011,** *45*, 2496-2506.

43. Breck, D. W., *Zeolite Molecular Sieves. Structure, Chemistry, and Use*. Wiley: 1973.

44. Li, Y. Y.; Perera, S. P.; Crittenden, B. D.; Bridgwater, J., The Effect of the Binder on the Manufacture of a 5A Zeolite Monolith. *Powder Technol.* **2001,** *116*, 85-96.

45. Whiting, G. T.; Chowdhury, A. D.; Oord, R.; Paalanen, P.; Weckhuysen, B. M., The Curious Case of Zeolite-clay/Binder Interactions and Their Consequences for Catalyst Preparation. *Faraday Discuss.* **2016,** *188*, 369-386.

46. Sulaymon, A. H.; Mahdi, A. S., Spherical Zeolite-Binder Agglomerates. *Chem. Eng. Res. Des.* **1999,** *77*, 342-350.

47. Antonides, L. E., *Diatomite, 1997, US Geological Survey (https://s3-us-west-2.amazonaws.com/prd-wret/assets/palladium/production/mineral-pubs/diatomite/250497.pdf), accessed on May 26, 2019.*

48. Parker, J. I.; Conway, H. L.; Yaguchi, E. M., Dissolution of Diatom Frustules and Recycling of Amorphous Silicon in Lake Michigan. *J. Fish Res. Board Can.* **1977,** *34*, 545-551.

49. Palomino, A. M.; Kim, S.; Summitt, A.; Fratta, D., Impact of diatoms on fabric and chemical stability of diatom–kaolin mixtures. *Appl. Clay Sci.* **2011,** *51*, 287-294.

50. *Silica Flour, US Silica (http://www.ussilica.com/sites/ussilica.com/files/US-Silica-Flour-USM-200.pdf), accessed on October 3, 2017.*

51. Russell, H. H.; Matthews, J. E.; Sewell, G. W. *TCE removal from contaminated soil and ground water. Ground water issue*; Environ. Protect. Agency: 1992; p 12.

52. Bangi, U. K. H.; Parvathy Rao, A.; Hirashima, H.; Venkateswara Rao, A., Physico-chemical Properties of Ambiently Dried Sodium Silicate Based Aerogels Catalyzed with Various Acids. *J. Sol-Gel Sci. Technol.* **2009,** *50*, 87-97.

53. Essien, E. R.; Olaniyi, O.; Adams, L. A.; Shaibu, R. O.; Chukwu, T., Method for Modifying the Morphology of Silica Particles Derived from Sodium Metasilicate. *Mater. Sci. Ind. J.* **2014,** *10*, 199-204.

54. *Web searches on July 16, 2019 showed that, for example, the tonnage prices of zeolite, diatomite and silica flour were $140-300 (https://www.alibaba.com/product-detail/Zeolite-3A-4A-5A-and13-*

X_60759771903.html?spm=a2700.7724857.normalList.184.4b0d5af9c04DQ7), $300 (https://www.alibaba.com/product-detail/Best-Market-Diatomite-price_60428262854.html?spm=a2700.7724857.normalList.80.140b4bf5wU5aF5) and $150 (https://www.kemcore.com/silica-flour-quartz-powder-99.html), respectively.

55. Allan, D., Sodium Peroxodisulfate. *Acta Crystallogr. E* **2006,** *62*, i44-i46.

56. de la Calle, R. G.; Gimeno, O.; Rivas, J., Percarbonate as a Hydrogen Peroxide Carrier in Soil Remediation Processes. *Environ. Eng. Sci.* **2012,** *29*, 951-956.

57. Jiang, W.; Tang, P.; Lu, S.; Xue, Y.; Zhang, X.; Qiu, Z.; Sui, Q., Comparative studies of H2O2/Fe(II)/formic acid, sodium percarbonate/Fe(II)/formic acid and calcium peroxide/Fe(II)/formic acid processes for degradation performance of carbon tetrachloride. *Chem. Eng. J.* **2018,** *344*, 453-461.

58. Zang, X.; Gu, X.; Lu, S.; Miao, Z.; Zhang, X.; Fu, X.; Fu, G. Y.; Qiu, Z.; Sui, Q., Enhanced degradation of trichloroethene by sodium percarbonate activated with Fe(II) in the presence of citric acid. *Water Supply* **2016,** *17*, 665-673.

59. Lee, E. S.; Seol, Y.; Fang, Y. C.; Schwartz, F. W., Destruction Efficiencies and Dynamics of Reaction Fronts Associated with the Permanganate Oxidation of Trichloroethylene. *Environ Sci Technol* **2003,** *37*, 2540-2546.

60. Yuan, B.; Chen, Y.; Fu, M.-L., Degradation efficiencies and mechanisms of trichloroethylene (TCE) by controlled-release permanganate (CRP) oxidation. *Chem. Eng. J.* **2012,** *192*, 276-283.

61. Fong, J. K.; Pena, J. K.; Xue, Z.-L.; Alam, M. M.; Sampathkumaran, U.; Goswami, K., Optical Sensors for the Detection of Trace Chloroform. *Anal. Chem.* **2015,** *87*, 1569-1574.

62. Dansby-Sparks, R. N.; Jin, J.; Mechery, S. J.; Sampathkumaran, U.; Owen, T. W.; Yu, B. D.; Goswami, K.; Hong, K.; Grant, J.; Xue, Z.-L., Fluorescent-Dye-Doped Sol−Gel Sensor for Highly Sensitive Carbon Dioxide Gas Detection below Atmospheric Concentrations. *Anal. Chem.* **2010,** *82*, 593-600.

63. Fong, J.; Dansby-Sparks, R.; Lamb, A.; Owen, T.; Mushfiq, M.; Sampathkumaran, U.; Goswami, K.; Jensen, S.; Xue, Z., Fluorescent-Dye Doped Thin-Film Sensors for the Detection of Alcohol Vapors. *Am. J. Anal. Chem.* **2014,** *5*, 566-580.

64. Federico-Perez, R. A.; Xue, Z.-L., Optical probe for the analysis of trace indole in shrimp. *Anal. Biochem.* **2018,** *557*, 104-110.

65. Liang, C.; Huang, C.-F.; Mohanty, N.; Kurakalva, R. M., A Rapid Spectrophotometric Determination of Persulfate Anion in ISCO. *Chemosphere* **2008,** *73*, 1540-1543.

66. Yuan, S.; Liao, P.; Alshawabkeh, A. N., Electrolytic manipulation of persulfate reactivity by iron electrodes for trichloroethylene degradation in groundwater. *Environ Sci Technol* **2014,** *48*, 656-663.

67. US Environmental Protection Agency. Method 551.1 Determination of Chlorination Disinfection Byproducts, Chlorinated Solvents, and Halogenated Pesticides/Herbicides in Drinking Water by Liquid-Liquid Extraction and Gas Chromatography with Electron Capture Detection. **1995**.

68. Sing, K. S. W., Adsorption methods for the characterization of porous materials. *Adv. Colloid Interface Sci.* **1998,** *76-77*, 3-11.

Vita

Peter Pham was born in New Orleans, Louisiana. He graduated from Eleanor McMain Secondary School in 2011. Shortly after, Peter attended Xavier University of Louisiana and received his Bachelors of Science degree in Chemistry in Spring 2015. During his senior year here, he performed organic chemistry research under the guidance of Dr. Maryam Foroozesh. After graduating with his B.S. degree, Peter continued his research as a BUILD lab technician until Summer 2016 before enrolling into UTK in Fall 2016.